Electronic Supplementary Information (ESI) for New Journal of Chemistry
This journal is (c) The Royal Society of Chemistry 2022

Supplementary Information

Efficient all-small-molecule organic solar cells based on a fluorinated small-molecule donor

Nailiang Qiu[1]*, Chunyan Liu[1,2], Haijiao Lang[1], Jingyang Xu[1], Rui Su[1], Jie Jiang[1], Jiaqi Tian[1], Jisen Li[1]*

[1]School of Chemistry, Chemical Engineering and Materials, Jining University, Qufu, China.

[2]School of Materials Science & Engineering, Tianjin Key Laboratory for Photoelectric Materials and Devices, Key Laboratory of Display Materials & Photoelectric Devices, Ministry of Education, Tianjin University of Technology, Tianjin, China.

*Corresponding authors.

E-mail: nlqiu@jnxy.edu.cn (N Qiu); senjili@sina.com (J Li)

Materials and synthesis of BTEHR-FT

All reactions and manipulations were carried out using standard Schlenk techniques under argon atmosphere. The solvents were purified and dried according to standard procedures. The non-fullerene acceptor F-2Cl was prepared according to the reported procedure.[1] Compound 1 and 2 were purchased from Woerjiming (Beijing) Technology Development Institute. The other materials were commercially available and used without further purification.

Compound **3**: Under the protection of argon, the weighed compound **1** (0.40 g, 0.43 mmol), compound **2** (0.54 g, 0.93 mmol) and $Pd(PPh_3)_4$ (30 mg) were placed into the dehydrated toluene (25 mL). And the reaction solution was stirred for 24 h at 110 ^oC under dark condition. After removing the solvent, the crude product was purified by silica gel chromatography using petroleum ether/dichloromethane (1:1.5, v/v) as the eluent. Finally, the pure compound **3** was obtained as a red solid (0.57 g, 83%). ^1H NMR (400 MHz, $CDCl_3$), δ (ppm): 9.83 (s, 2H), 7.60 (s, 4H), 7.24 (s, 2H), 7.17 (s, 4H), 7.14 (s, 2H), 7.13 (s, 2H), 2.82-2.75 (m, 12H), 1.71-1.68 (m, 10H), 1.45-1.25 (m, 56H), 1.01-0.86 (m, 24H). ^{13}C NMR (100 MHz, $CDCl_3$), δ (ppm): 183.74, 155.62, 153.11, 146.94, 146.47, 143.13, 141.48, 139.26, 138.90, 138.52, 137.77, 137.08, 135.79, 135.46, 133.95, 128.33, 126.07, 125.64, 124.36, 123.06, 120.83, 118.14, 41.35, 40.71, 34.38, 32.63, 32.58, 29.68, 29.53, 28.93, 28.87, 28.82, 25.89, 25.86, 25.75, 25.71, 23.09, 23.06, 19.79, 14.18, 10.87. MALDI-TOF MS: calcd for $C_{92}H_{116}F_2O_2S_{10}$ $[M+H]^+$, 1611.62; found: 1611.89.

BTEHR-FT: The compound **3** (120 mg, 0.074 mmol) and 3-(2-ethylhexyl)rhodanine (182.6 mg, 0.74 mmol) were dissolved in dry $CHCl_3$ (15 mL), and then the solution was deoxygenated using argon gas for 10 min. Subsequently, dry piperidine (0.1 mL) was added by syringe and the reaction solution was heated to 60 °C. After stirring for 15 h, the mixture was poured into water (100mL) and extracted using $CHCl_3$ (50 mL × 3). The combined organic layer was washed twice using water and then dried by anhydrous Na_2SO_4. After removal of solvent, the crude product was chromatographied by silica gel using petroleum ether/$CHCl_3$ (1:2, v/v) as the eluent, yielding a powdery dark purple solid (131.6 mg, 86%). ^{1}H NMR (400 MHz, $CDCl_3$), δ (ppm): 7.67 (s, 2H), 7.50 (t, 2H), 7.16 (d, 6H), 7.05 (d, 4H), 3.97 (d, 4H), 2.86 (d, 4H), 2.76-2.73 (m, 8H), 2.05-2.03 (m, 2H), 1.74-1.66 (m, 10H), 1.41-1.26 (m, 72H), 1.02-0.88 (m, 36H). ^{13}C NMR (100 MHz, $CDCl_3$), δ (ppm): 192.54, 167.91, 155.60, 153.06, 140.86, 139.37, 138.43, 137.78, 137.36, 137.13, 135.12, 135.01, 134.82, 133.87, 133.77, 130.84, 128.49, 127.07, 126.04, 124.64, 122.60, 122.47, 122.29, 120.33, 118.09, 117.81, 48.69, 40.88, 37.02, 32.56, 31.94, 31.91, 31.44, 30.53, 30.43, 30.20, 29.85, 29.78, 29.71, 29.63, 29.53, 29.49, 29.49, 29.36, 29.32, 28.90, 28.47, 25.90, 23.93, 23.11, 23.01, 22.70, 14.26, 14.14, 14.07, 10.95, 10.55. MS (MALDI-TOF): calcd for $C_{114}H_{150}F_2N_2O_2S_{14}$ $[M+H]^+$, 2065.78, found: 2065.70.

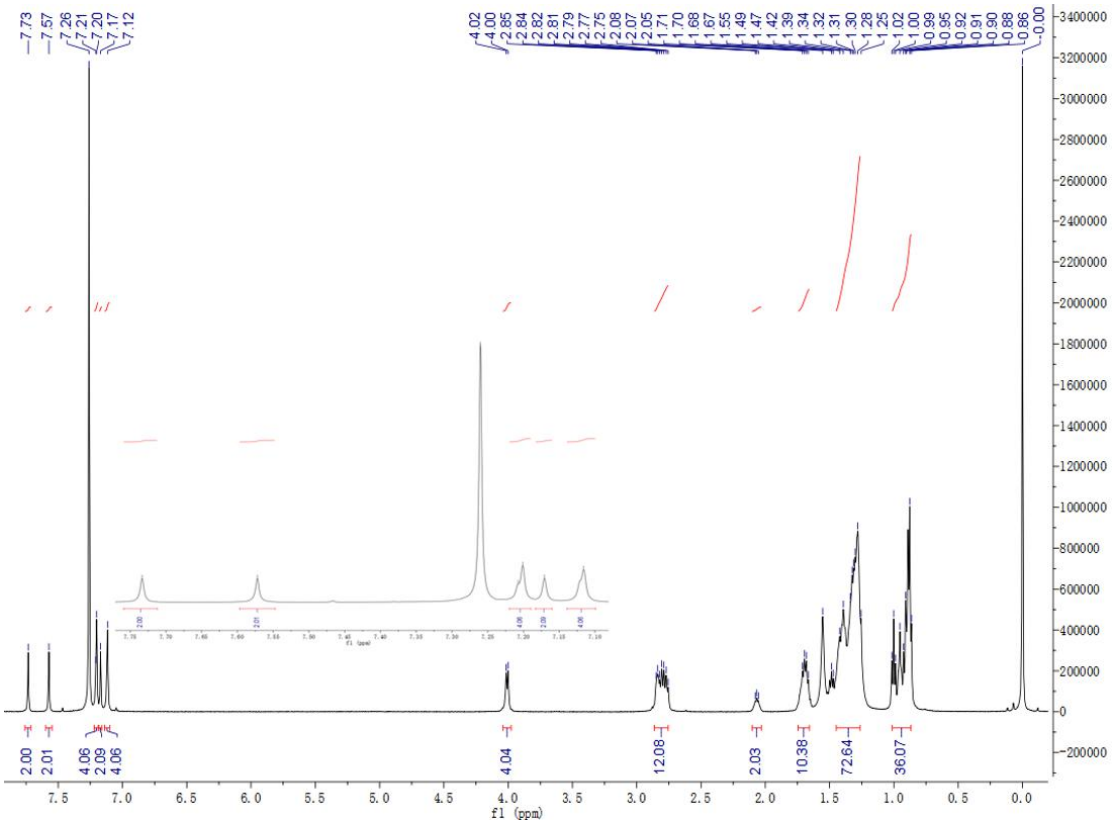

Fig. S1 ^{1}H NMR spectra of compound BTEHR-FT at 300K in $CDCl_3$.

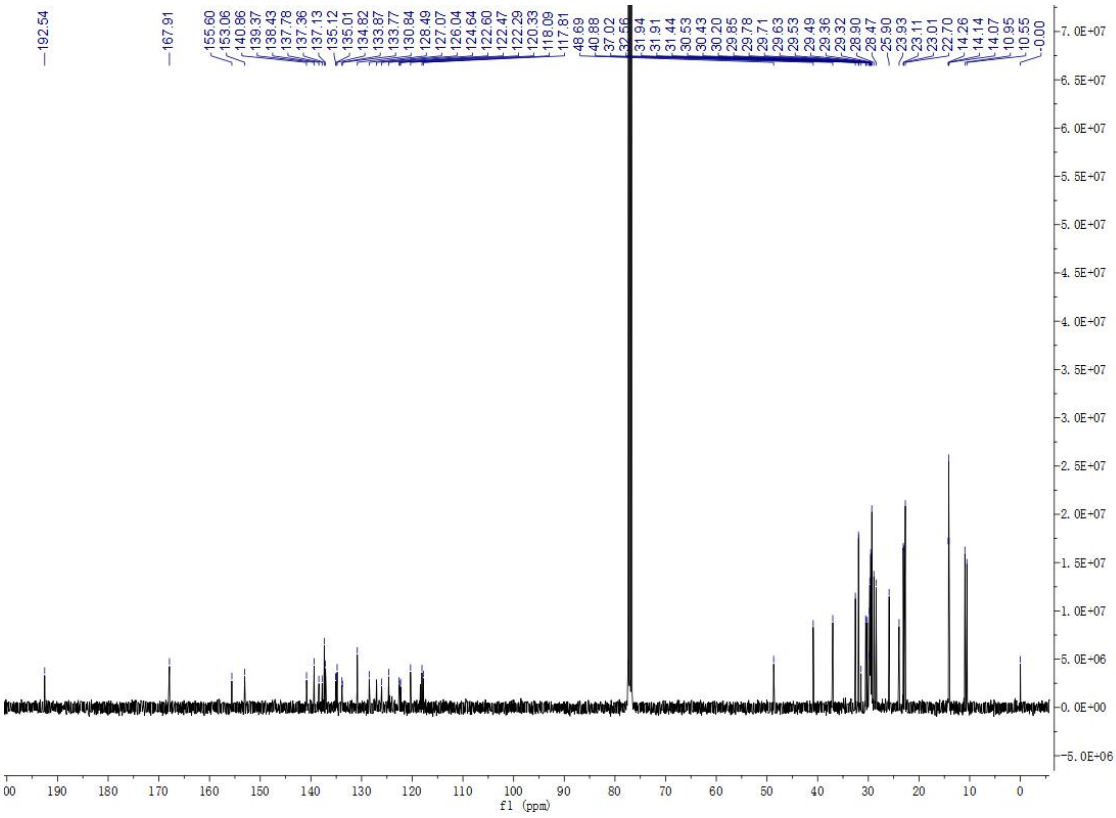

Fig. S2 ^{13}C NMR spectra of compound BTEHR-FT at 300K in $CDCl_3$.

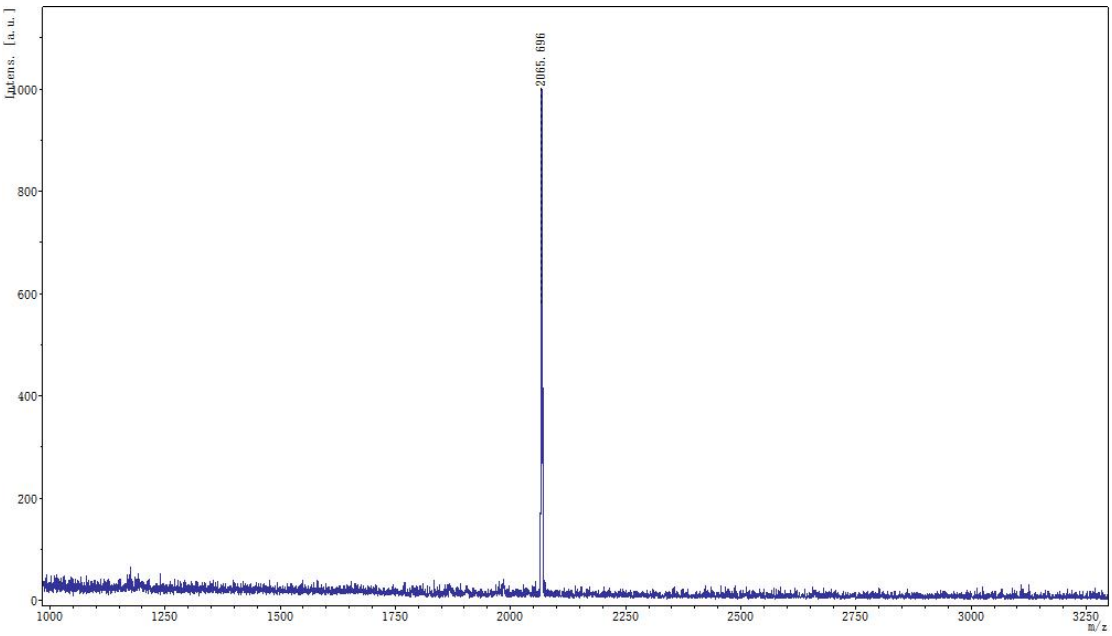

Figure S3 The MALDI-TOF MS plot of compound BTEHR-FT.

Measurements and Instruments

The ^{1}H and ^{13}C nuclear magnetic resonance (NMR) spectra were obtained using a Bruker AV400 Spectrometer. Matrix assisted laser desorption/ionization time-of-flight (MALDI-TOF) mass spectrometry were performed on a Bruker Autoflex III instrument. The thermogravimetric analysis (TGA) was carried out on a NETZSCH STA 449 F5 Jupiter instrument with the heating rate of 10 °C min^{-1} under purified nitrogen gas flow. UV-vis spectra were obtained with a JASCO V-570 spectrophotometer. X-ray diffraction (XRD) experiments were performed on a Bruker Model D8 FOCUS X-ray diffractometer with Cu Kα radiation (λ = 1.5406 Å) at a generator voltage of 40 kV and a current of 40 mA. Cyclic voltammetry (CV) experiments were performed with a LK98B II Microcomputer-based Electrochemical Analyzer in acetonitrile solution. All measurements were carried out at room

temperature with a conventional three-electrode configuration using a glassy carbon electrode as the working electrode, a saturated calomel electrode (SCE) as the reference electrode, and a platinum wire as the counter electrode. Tetrabutylammonium phosphorus hexafluoride (*n*-Bu_4NPF_6, 0.1 M) in acetonitrile was used as the supporting electrolyte, and the scan rate was 100 mV s^{-1}. The Differential scanning calorimetry (DSC) measurement was carried out on a Setline STA instrument with the heating rate of 10 °C min^{-1} under purified nitrogen gas flow. The photoluminescence (PL) measurements were performed by the HORIBA Scientific Fluorolog-3 instrument.

The current density-voltage (*J-V*) characteristics of ASM-OSC devices were measured with a Keithley 2400 source-measure unit. Using a SAN-EI XES-70S1 AAA class solar simulator, photocurrent was performed under illumination with simulated 100 mW cm^{-2} AM 1.5G irradiation. The external quantum efficiency (EQE) curve was obtained by a QE-R Solar Cell Spectral Response Measurement System. The film thicknesses were parallel tested by VeecoDektak 150 profilometer.

Space charge limited current (SCLC) mobility was performed by a diode configuration of ITO/ZnO/active layer/Al for electron mobility and ITO/PEDOT:PSS/active layer/Au for hole mobility, respectively. The results were fitted via a space charge limited form, being described as the equation:

$$J = \frac{9\varepsilon_0\varepsilon_r\mu_0 V^2}{8L^3}\exp\left(0.89\beta\sqrt{\frac{V}{L}}\right)$$

where J is the current density, ε_0 is the permittivity of free space (8.85 × 10^{-12} F m^{-1}), ε_r is the relative dielectric constant of the transport medium, μ_0 is the hole or

electron mobility, V (= V_{appl} − V_{bi}) is the internal voltage in the device, where V_{appl} is the applied voltage to the device and V_{bi} is the built-in voltage due to the relative work function difference of the two electrodes, L is the film thickness of the active layer. Atomic force microscopy (AFM) and Transmission electron microscopy (TEM) images were obtained on a Bruker MultiMode 8 in tapping mode and Philips Technical G2 F20 at 200 kV, respectively.

Fabrication of ASM-OSC devices

The ASM-OSC devices were fabricated with conventional structure of ITO/PEDOT:PSS/avtive layer/PDINO/Al as the following procedures. The ITO-coated glasses were cleaned using a detergent scrub, and subsequently subjected to ultrasonic treatment in soap water, deionized water, acetone and isopropyl alcohol for 15 min in each step. After drying by a nitrogen flow, the ITO substrates were treated by ultraviolet-ozone for 15 min and spin-coated with PEDOT:PSS solution at 4800 rpm for 20 s. Subsequently, the glasses were baked at 150 °C for 20 min and transferred into the glove box with argon gas. Chloroform solution of both donor (8.0 mg/mL) and acceptor (7.2 mg/mL for D/A weight ratio of 1:0.9) was spin-coated on the PEDOT:PSS at 1800 rpm for 20 s, and then annealed on the hot plate at 90 °C for 5 min (TA) or in the chloroform solvent vapor for 60 s (SVA). Afterward, PDINO with the concentration of 1.0 mg/mL using EtOH as solvent was spin-coated on the active layer at 3000 rpm for 20s. Finally, under the high vacuum, a cathode material Al was deposited onto PDINO layer. The work area of each device is about 0.04 cm^2, defined by the masks for all the solar cell devices discussed in this work.

Table S1 Photovoltaic performances of the devices based on BTEHR-FT (D):F-2Cl (A) with different weight ratio under various optimization conditions.

D:A (w/w)	Treatment	V_{oc} (V)	J_{sc} (mA cm^{-2})	FF	PCE$_{max}$ (%)[a]
1:0.8	As cast	0.953	11.54	0.633	6.96 (6.75 ± 0.21)
1:0.9	As cast	0.948	12.10	0.658	7.55 (7.26 ± 0.29)
1:1.0	As cast	0.943	12.13	0.628	7.18 (7.05 ± 0.13)
1:0.9	SVA(CF, 60s)	0.889	12.04	0.691	7.39 (7.15 ± 0.24)
1:0.9	SVA(THF, 80s)	0.885	11.88	0.679	7.14 (7.02 ± 0.12)
1:0.9	TA(70℃, 10min)	0.931	15.30	0.678	9.66 (9.42 ± 0.24)
1:0.9	TA(90℃, 5min)	0.932	16.59	0.693	10.71 (10.45 ± 0.26)
1:0.9	TA(100℃, 5min)	0.928	15.98	0.692	10.26 (10.01 ± 0.25)
1:0.9	TA(110℃, 5min)	0.911	15.78	0.680	9.77 (9.47 ± 0.30)

[a] Average PCE values obtained from 10 devices are shown in parentheses.

Table S2 Photovoltaic performances of the devices based on the as cast BTEHR-FT:F-2Cl (w/w, 1:0.9) films under different rotation speed.

Rotation speed (rpm)	V_{oc} (V)	J_{sc} (mA cm^{-2})	FF	PCE$_{max}$ (%)[a]
1500, 20s	0.951	11.50	0.632	6.91 (6.66 ± 0.25)
1700, 20s	0.950	11.81	0.649	7.28 (6.97 ± 0.31)
1800, 20s	0.948	12.10	0.658	7.55 (7.26 ± 0.29)
1900, 20s	0.942	11.89	0.655	7.33 (7.08 ± 0.25)

[a] Average PCE values obtained from 10 devices are shown in parentheses.

Table S3 Photovoltaic performances of the devices based on the BTEHR-FT:F-2Cl (w/w, 1:0.9). The blend films were cast under different rotation speed, and then treated by 90 ℃ for 5 min.

Rotation speed (rpm)	V_{oc} (V)	J_{sc} (mA cm^{-2})	FF	PCE$_{max}$ (%)[a]
1700, 20s	0.939	16.13	0.685	10.37 (10.03 ± 0.34)

1800, 20s	0.932	16.59	0.693	10.71 (10.45 ± 0.26)
1900, 20s	0.930	15.94	0.688	10.20 (9.91 ± 0.29)

[a] Average PCE values obtained from 10 devices are shown in parentheses.

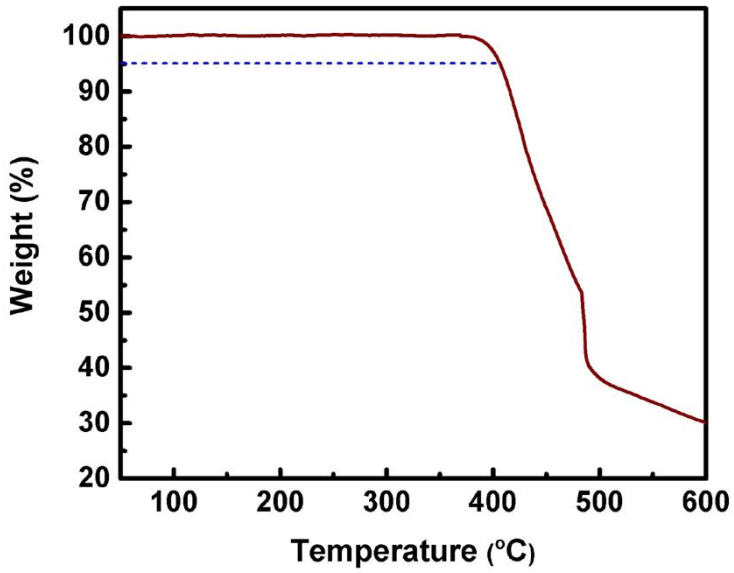

Fig. S4 Thermogravimetric analysis plot of BTEHR-FT with a heating rate of 10 °C min^{-1}.

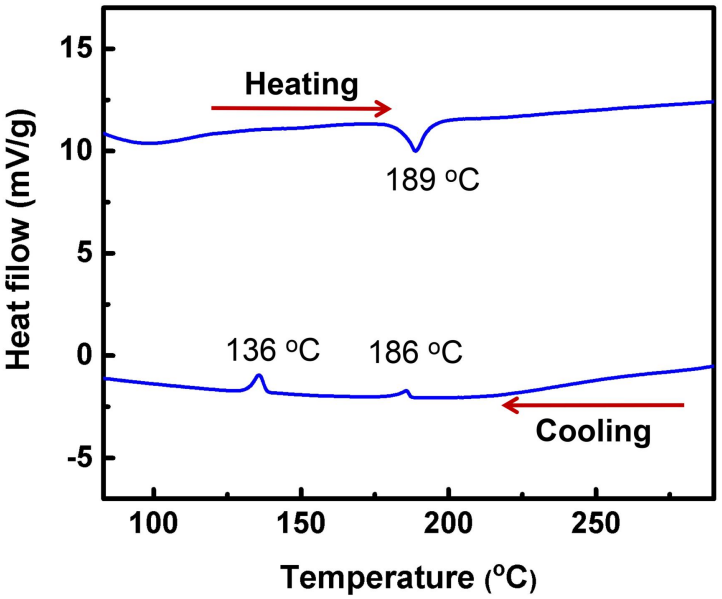

Fig. S5 DSC curves of BTEHR-FT at a scan rate of 10 °C min^{-1} under nitrogen.

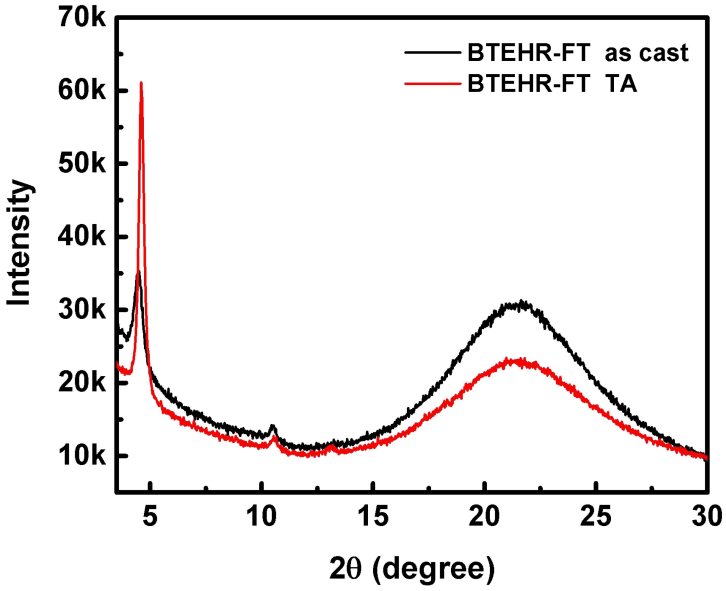

Fig. S6 XRD patterns of BTEHR-FT films without/with thermal annealing at 90 ℃ for 5 min.

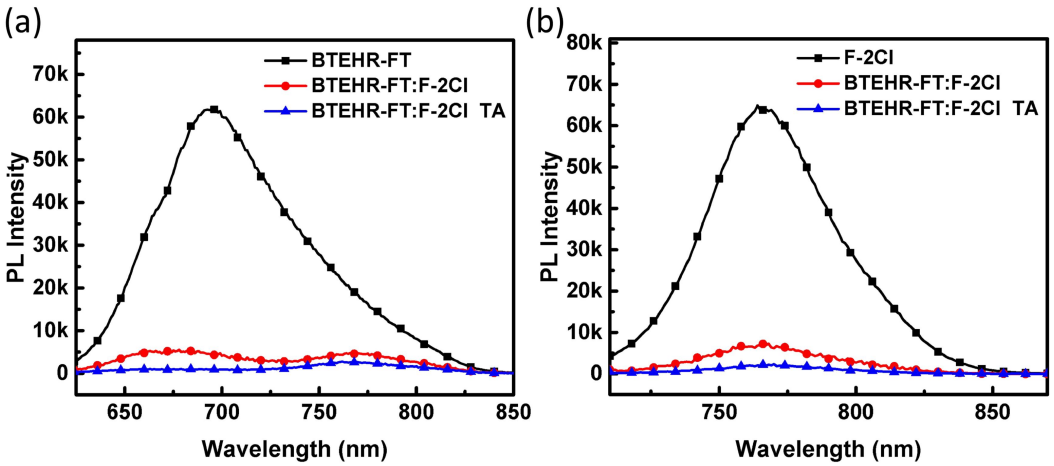

Fig. S7 Photoluminescence (PL) spectra of (a) BTEHR-FT and the related blend films excited at 560 nm and (b) F-2Cl and the related blend films excited at 700 nm.

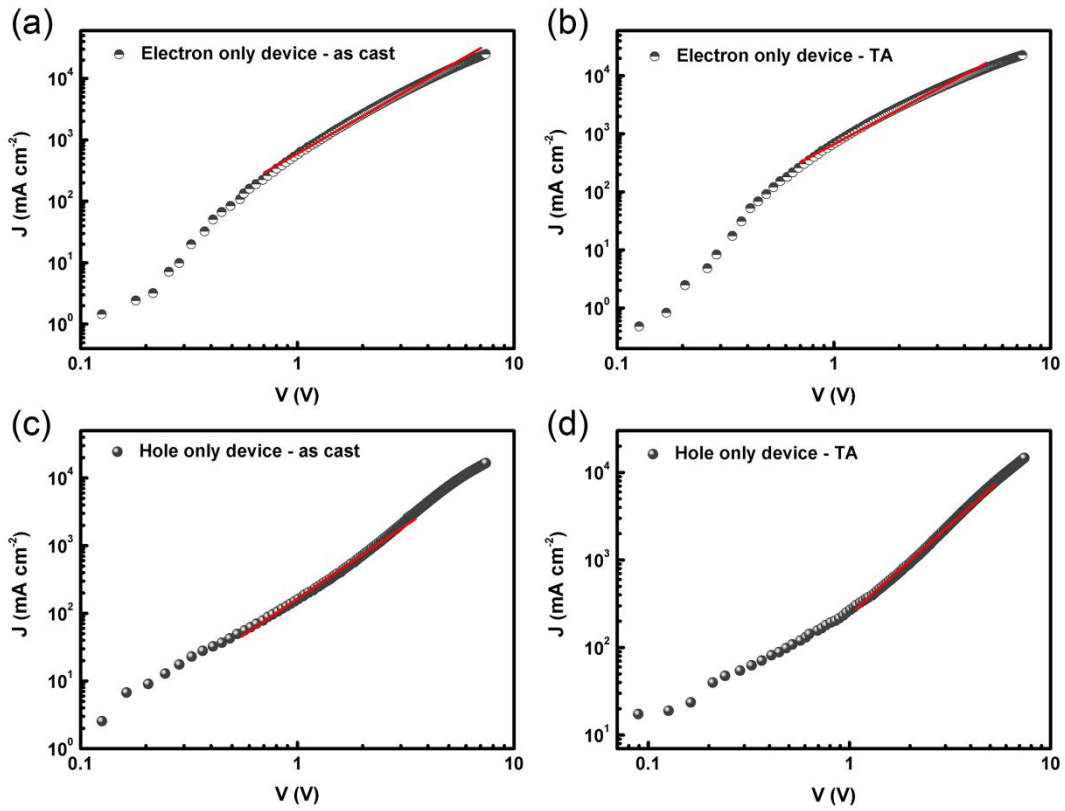

Fig. S8 The current density-voltage (*J-V*) plots for electron-only devices based on BTEHR-FT:F-2Cl with (a) as cast and (b) thermal annealing (TA), and hole-only devices based on BTEHR-FT:F-2Cl with (c) as cast and (d) TA.

References

1. Y. Wang, M. Chang, B. Kan, X. Wan, C. Li and Y. Chen, *ACS Appl. Mater. Interfaces*, 2018, **1**, 2150-2156.